DIASSOCIATIVE ALGEBRAS AND MILNOR'S INVARIANTS FOR TANGLES

OLGA KRAVCHENKO AND MICHAEL POLYAK

ABSTRACT. We extend Milnor's μ-invariants of link homotopy to ordered (classical or virtual) tangles. Simple combinatorial formulas for μ-invariants are given in terms of counting trees in Gauss diagrams. Invariance under Reidemeister moves corresponds to axioms of Loday's diassociative algebra. The relation of tangles to diassociative algebras is formulated in terms of a morphism of corresponding operads.

1. INTRODUCTION

The theory of links studies embeddings of several disjoint copies of S^1 into $\mathbb{R}^3$ and thus has to deal with a mixture of linking and self-knotting phenomena. The theory of link-homotopy was developed by Milnor [7] in order to isolate the linking phenomena from the self-knotting ones and to study linking separately. A fundamental set of link-homotopy invariants is given by Milnor's $\bar{\mu}_{i_1\dots i_r,j}$ invariants [7] with non-repeating indices $1 \leq i_1, \dots i_r, j \leq n$. Roughly speaking, these describe the dependence of the j-th parallel on the meridians of the $i_1, \dots, i_r$ components. The simplest invariant $\bar{\mu}_{i,j}$ is just the linking number of the corresponding components. The next one, $\bar{\mu}_{i_1 i_2,j}$, detects Borromean-type linking of the corresponding 3 components and together with the linking numbers classify 3-component links up to link-homotopy.

There is no semi-group structure defined on multi-component links such as one existing for knots. Namely, connected sum, while well-defined for knots, is not defined for links. On the level of invariants, this is manifested by a complicated recurrent indeterminacy in the definition of the $\bar{\mu}$-invariants (reflected in the use of notation $\bar{\mu}$, rather than μ). Introduction of string links in [3] remedied this situation, since connected sum is well-defined for string links. A version of $\bar{\mu}$-invariants modified for string links is thus free of the original indeterminacy; to stress this fact, we use the notation μ for these invariants from now on. Milnor's invariants classify string links up to link-homotopy ([3]).

1.1. **Brief statement of results.** Tangles generalize links, braids and string links. We define Milnor's $\mu-$invariants for tangles with ordered components along the lines of Milnor's original definition, that is in terms of generators of the (reduced) fundamental group of the complement of a tangle in a cylinder, using the Magnus expansion.

On the other hand, tangles may be encoded by Gauss diagrams (see [10, 2]). We follow the philosophy of [10] to define invariants of classical or virtual tangles

2010 *Mathematics Subject Classification.* 57M25; 57M27; 18D50; 16S37.

Key words and phrases. tangles, μ-invariants, planar trees, dialgebras, operads.

The second author was partially supported by the ISF grant 1343/10.

by counting (with appropriate weights and signs) certain subdiagrams of a Gauss diagram. Since subdiagrams used in computing these invariants correspond to rooted planar binary trees, we call the resulting invariants Z_j *tree invariants*.

Invariance of tangle diagrams under Reidemeister moves gives rise to several equivalence relations among the corresponding trees. We study these relations and find (Theorem 3.3) that they could be interpreted as defining relations of a diassociative algebra. The notion of diassociative algebra was introduced by Loday [6]. A diassociative algebra is a vector space with two associative operations – left and right multiplications. The five defining axioms (equation 2) of diassociative algebra describe invariance under the third Reidemeister move.

We explicitly write out the linear combinations of trees used in computing invariants of degrees 2,3 and 4. In particular, tree invariants $Z_{12,3}$ and $Z_{123,4}$ are computed and subsequently shown to coincide with the corresponding Milnor $\mu-$invariants.

Then we discuss the properties of tree invariants of (classical or virtual) tangles. In particular, we study their dependence on orderings and orientations of strings. Moreover, we show that these invariants satisfy certain skein relations, reminiscent of those satisfied by the Conway polynomial and the Kauffman bracket. The skein relations for Milnor invariants were determined by the second author in [8]. Similarity of skein relations of tree invariants to Milnor's invariants allows us to show that tree invariants $Z_{i_1\dots i_r,j}$ coincide with Milnor's μ-invariants $\mu_{i_1\dots i_r,j}$ when $1 \le j < i_1 < \dots < i_r \le n$. This also allows us to extend Milnor's μ-invariants to virtual tangles.

To describe the operadic structure on tangles we introduce the notion of a tree tangle. For tree tangles there is an appropriate operation of grafting, which allows us to define the operad of tree tangles. We show that there is a map from tangles to tree tangles by an operation called *capping*. We describe a morphism of operads between the operad of tree tangles and the diassociative algebra operad *Dias*.

The paper is organized in the following way. In Section 2 the main objects and tools are introduced: tangles, Milnor's μ-invariants, and Gauss diagram formulas. In Section 3 we review diassociative algebras and introduce tree invariants of tangles and prove their invariance under Reidemeister moves. Section 4 is devoted to the properties of the invariants and their identification with the μ-invariants. Finally, in Section 5 we discuss the operadic structure on tree tangles and the corresponding morphism of operads.

The authors are grateful to Paul Bressler, Frédéric Chapoton and Jean-Louis Loday for stimulating discussions, and to the French consulate in Israel for a generous travel support.

2. Preliminaries

2.1. **Tangles and string links.** Let D^2 be the unit disk in xy-plane and let p_i, $i = 1, \dots, N$ be some prescribed points in the interior of D^2. For definiteness, we can chose the disk to have the center at $(1, 0)$ and the points lying on the x-axis.

Definition 2.1. An (ordered, oriented) (k, l)-*tangle* without closed components in the cylinder $C = D^2 \times [0, 1]$ is an ordered collection of $n = \frac{1}{2}(k + l)$ disjoint oriented intervals, properly embedded in C in such a way, that the endpoints of each embedded interval belong to the set $\{p_i\}_{i=1}^k \times \{1\} \cup \{p_i\}_{i=1}^l \times \{0\}$ in C. See

Figure 1a. We will call embedded intervals the *strings* of a tangle. Tangles are considered up to an oriented isotopy in C, fixed on the boundary.

We will always assume that the only singularities of (the image of) the projection of a tangle to the xz-plane are transversal double points. Such a projection, equipped with the indication of over- and underpasses in each double point, is called a *tangle diagram*. See Figure 1b.

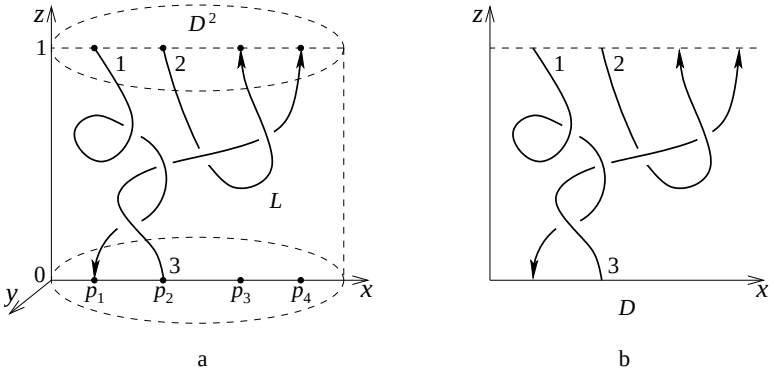

FIGURE 1. A $(4,2)$-tangle and its diagram

String links form an important class of tangles which is comprised by (n,n)-tangles such that the i-th arc ends in the points $p_i \times \{0,1\}$, see Figure 2a. By the *closure* $\widehat{L}$ of a string link L we mean the braid closure of L. It is an n-component link obtained from L by an addition of n disjoint arcs in the xz-plane, each of which meets C only at the endpoints $p_i \times \{0,1\}$ of L, as illustrated in Figure 2b. The linking number lk of two strings of L is their linking number in $\widehat{L}$. Two tangles are

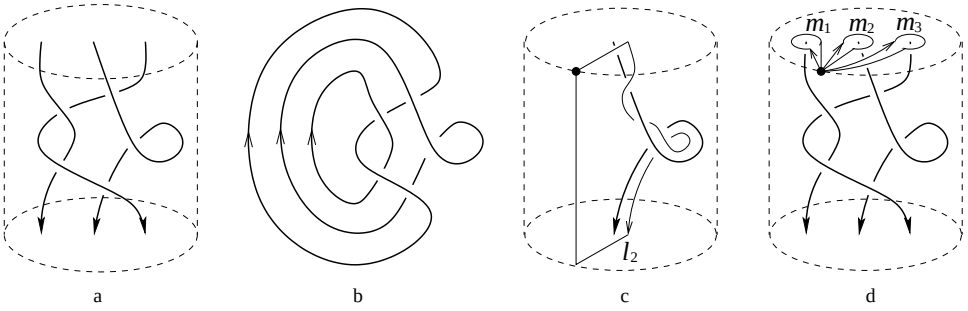

FIGURE 2. A string link, its closure, and canonical meridians and parallels

link-homotopic, if one can be transformed into the other by homotopy, which fails to be isotopy only in a finite number of instants, when a (generic) self-intersection point appears on one of the arcs.

2.2. **Milnor's μ-invariants.** Let us briefly recall the construction of Milnor's link-homotopy μ-invariants (see [7] for details, [5] for a modification to string links, and [8] for the case of tangles). We will first describe the well-studied case of string links, and then indicate modifications needed for the general case of tangles.

Let $L = \cup_{i=1}^n L_i$ be an n-component string link and consider the link group $\pi = \pi_1(C \smallsetminus L)$ with the base point $(1,1,1)$ on the upper boundary disc $D^2 \times \{1\}$. Choose *canonical parallels* $l_j \in \pi$, $j = 1, \dots, n$ represented by curves going parallel to L_j and then closed up by standard non-intersecting curves on the boundary of C so that $\mathrm{lk}(l_j, L_j) = 0$; see Figure 2c. Also, denote by $m_i \in \pi$, $i = 1, \dots, n$ the *canonical meridians* represented by the standard non-intersecting curves in $D^2 \times \{1\}$ with $\mathrm{lk}(m_i, L_i) = +1$, as shown in Figure 2d. If L is a braid, these meridians freely generate π, with any other meridian of L_i in π being a conjugate of m_i. For general string links, similar results hold for the reduced link group $\tilde{\pi}$.

Given a finitely-generated group G, the *reduced group* $\tilde{G}$ is the quotient of G by relations $[g, w^{-1}gw] = 1$, for any $g, w \in G$. One can show (see [3]) that $\tilde{\pi}$ is generated by m_i, $i = 1, \dots, n$ proceeding similarly to the usual construction of Wirtinger's presentation. Let F be the free group on n generators $x_1, \dots x_n$. The map $F \to \pi$ defined by $x_i \mapsto m_i$ induces the isomorphism $\widetilde{F} \cong \tilde{\pi}$ of the reduced groups [3]. We will use the same notation for the elements of π and their images in $\tilde{\pi} \cong \widetilde{F}$.

Now, let $\mathbb{Z}[[X_1, \dots, X_n]]$ be the ring of power series in n non-commuting variables X_i and denote by $\widetilde{Z}$ its quotient by the two-sided ideal generated by all monomials, in which at least one of the generators appears more than once. The *Magnus expansion* is a ring homomorphism of the group ring $\mathbb{Z}F$ into $\mathbb{Z}[[X_1, \dots, X_n]]$, defined by $x_i \mapsto 1 + X_i$, $x_i^{-1} \mapsto 1 - X_i + X_i^2 - \cdots$. It induces the homomorphism $\theta : \mathbb{Z}\widetilde{F} \to \widetilde{Z}$ of the corresponding reduced group rings. In particular, for the case of $\widetilde{F}$ being the link group of a link L there is the homomorphism of reduced group rings $\theta_L : \mathbb{Z}\tilde{\pi} \to \widetilde{Z}$.

Milnor's invariants $\mu_{i_1 \dots i_r, j}(L)$ of the string link L are defined as coefficients of the Magnus expansion $\theta_L(l_j)$ of the parallel l_j:

$$\theta_L(l_j) = \sum \mu_{i_1 \dots i_r, j} X_{i_1} X_{i_2} \dots X_{i_r} \ .$$

In particular, if L_j passes everywhere in front of the other components, all the invariants $\mu_{i_1 \dots i_r, j}$ vanish. Modulo lower degree invariants $\mu_{i_1 \dots i_r, j}(L) \equiv \bar{\mu}_{i_1 \dots i_r, j}(\widehat{L})$, where $\bar{\mu}_{i_1 \dots i_r, j}(\widehat{L})$ are the original Milnor's link invariants [7].

The above definition of invariants $\mu_{i_1 \dots i_r, j}(L)$ may be adapted to ordered oriented tangles without closed components in a straightforward way. The canonical meridian m_i of L_i is defined as a standard curve on the boundary of C, making a small loop around the starting point of L_i (with $\mathrm{lk}(m_i, L_i) = +1$). A canonical parallel l_j of L_j is a standard closure of a pushed-off copy of L_j (with $\mathrm{lk}(l_j, L_j) = 0$). See Figure 3. The only difference with the string link case is that for general tangles there is no well-defined canonical closure (some additional choices – e.g. of a marked component – are needed).

Remark 2.2. Note that the invariants $\mu_{i_1 \dots i_r, j}$ significantly depend on the order of indices $i_1, i_2, \dots, i_r$ and j (e.g., in general $\mu_{i_1 i_2 \dots i_r, j}(L) \neq \mu_{i_2 i_1 \dots i_r, j}(L)$). Under a permutation $\sigma \in S_n$, $\sigma : i \mapsto \sigma(i)$ μ-invariants change in an obvious way: $\mu_{i_1 i_2 \dots i_r, j}(L') = \mu_{\sigma(i_1)\sigma(i_2) \dots \sigma(i_r), \sigma(j)}(L)$, where L' is the tangle L with changed ordering: $L'_i = L_{\sigma(i)}$.

2.3. **Gauss diagrams.** Gauss diagrams provide a simple combinatorial way to encode links and tangles. Consider a tangle diagram D as an immersion $D : \sqcup_{i=1}^n I_i \to$

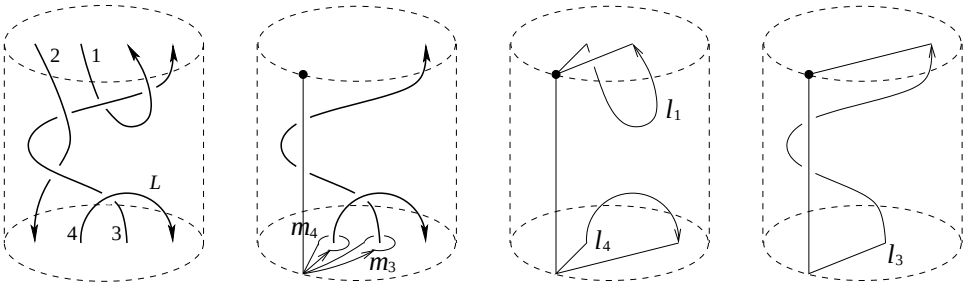

FIGURE 3. A choice of canonical meridians and parallels for a tangle

$\mathbb{R}^2$ of n disjoint copies of the unit interval into the xz-plane, equipped with information about the overpass and the underpass in each crossing.

Definition 2.3. Let L be a (k,l)-tangle and D its diagram. The *Gauss diagram* G corresponding to D is an ordered collection of $n = \frac{1}{2}(k+l)$ intervals $\sqcup_{i=1}^{n} I_i$ with the preimages of each crossing of D connected by an arrow. Arrows are pointing from the over-passing string to the under-passing string and are equipped with the sign: ± 1 of the corresponding crossing (its local writhe).

We will usually depict the intervals in a Gauss diagram as vertical lines, assuming that they are oriented downwards and ordered from left to right. See Figure 4.

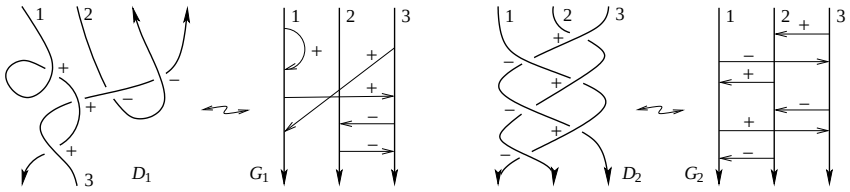

FIGURE 4. Gauss diagrams

The Gauss diagram of a tangle, G, encodes all the information about the crossings, and thus all the essential information contained in the tangle diagram D, in a sense that, given endpoints of each string, D can be reconstructed from G uniquely up to isotopy. Reidemeister moves of tangle diagrams may be easily translated into the language of Gauss diagrams, see Figure 5. Here fragments participating in a move may be parts of the same string or belong to different strings, ordered in an arbitrary fashion, and the fragments in $\Omega 1$ and $\Omega 2$ may have different orientations. It suffices to consider only one oriented move of type three, see [1, 9].

2.4. **Virtual tangles.** Note that not all collections of arrows connecting a set of n strings can be realized as a Gauss diagram of some tangle. Dropping this realization requirement leads to the theory of virtual tangles, see [4, 2]. We may simply define a virtual tangle as an equivalence class of virtual (that is, not necessary realizable) Gauss diagrams modulo the Reidemeister moves of Figure 5.

The fundamental group $\pi_1(C \setminus L)$ may be explicitly deduced from a Gauss diagram of a tangle L. It is easy to check that the fundamental group is invariant under the Reidemeister moves. Thus, the construction of Section 2.2 may be carried

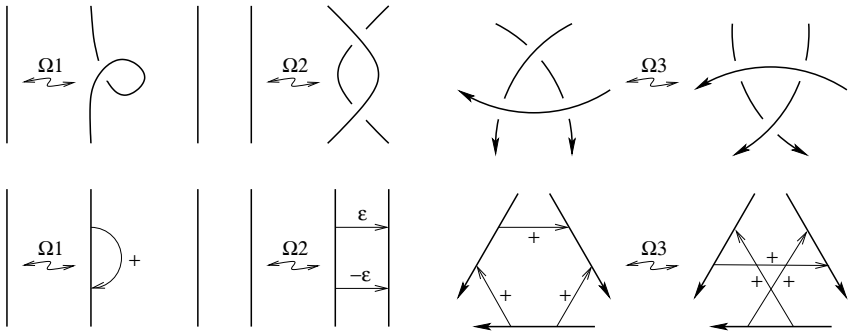

FIGURE 5. Reidemeister moves for diagrams and Gauss diagrams

out for virtual tangles as well, resulting in a definition of μ-invariants of virtual tangles.

The only new feature in the virtual case is the existence of two tangle groups. This is related to a possibility to choose the base point for the computation of the fundamental group $\pi = \pi_1(C \smallsetminus L)$ either in the front half-space $y > 0$ (see Figure 2 and Section 2.2), or in the back half-space $y < 0$. While for classical tangles Wirtinger presentations obtained using one of these base points are two different presentations of the same group π, for virtual tangles we get two different - the upper and the lower - tangle groups. See [2] for details. The passage from the upper to the lower group corresponds to a reversal of directions (but not of signs!) of all arrows in a Gauss diagram. Using the lower group in the construction of Section 2.2, we would end up with another definition of μ-invariants, leading to a different set of "lower μ-invariants" in the virtual case. We will return to this discussion in Remark 4.9 below.

2.5. **Gauss diagram formulas.**

Definition 2.4. An *arrow diagram on n strings* is an ordered set of n oriented intervals (strings), with several arrows connecting pairs of distinct points on intervals, considered up to orientation preserving diffeomorphism of the intervals.

See Figure 6. In other words, an arrow diagram is a virtual Gauss diagram in which we forget about realizability and signs of arrows.

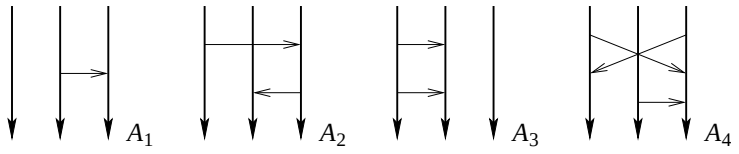

FIGURE 6. Arrow diagrams

Given an arrow diagram A on n strings and a Gauss diagram G with n intervals, we define a map $\phi : A \to G$ as an embedding of A into G which maps intervals to intervals and arrows to arrows, preserving their orientations and ordering of intervals. The sign of ϕ is defined as $\mathrm{sign}(\phi) = \prod_{a \in A} \mathrm{sign}(\phi(a))$. Finally, define a

pairing $\langle A, G\rangle$ as

$$\langle A, G\rangle = \sum_{\phi: A\to G} \mathrm{sign}(\phi)$$

and if there is no embedding of $A \to G$, then $\langle A, G\rangle = 0$. For example, for arrow diagrams A_1, A_2, A_3, A_4 of Figure 6 and Gauss diagrams G_1, G_2 shown in Figure 4, we have $\langle A_1, G_1\rangle = \langle A_2, G_1\rangle = \langle A_4, G_1\rangle = -1$, $\langle A_2, G_2\rangle = 1$ and $\langle A_3, G_1\rangle = \langle A_1, G_2\rangle = \langle A_3, G_2\rangle = \langle A_4, G_2\rangle = 0$. We extend $\langle \cdot, G\rangle$ to a vector space generated by all arrow diagrams on n strings by linearity.

For some special linear combinations A of arrow diagrams the expression $\langle A, G\rangle$ is preserved under the Reidemeister moves of G, thus resulting in an invariant of (ordered) tangles. See [10] and [2] for details and a general discussion on this type of formulas. The simplest example of such an invariant is a well-known formula for the linking number of two components:

$$\mathrm{lk}(L_1, L_2) = \langle \,|\!\!\leftarrow\!\!|\,, G\rangle. \tag{1}$$

The right hand side is the sum $\sum_{\phi: A\to G} \mathrm{sign}(\phi)$ over all maps of $A = |\!\!\leftarrow\!\!|$ to G. In other words, it is just the sum of signs of all crossings of D, where L_1 passes under L_2.

Remark 2.5. Note that for string links one has

$$\mathrm{lk}(L_1, L_2) = \langle \,|\!\!\leftarrow\!\!|\,, G\rangle = \langle \,|\!\!\rightarrow\!\!|\,, G\rangle = \mathrm{lk}(L_2, L_1).$$

For general tangles, however, these two invariants may differ. For example, for a tangle diagram with just one crossing, where L_1 passes in front of L_2, we have $\langle \,|\!\!\leftarrow\!\!|\,, G\rangle = 0$ and $\langle \,|\!\!\rightarrow\!\!|\,, G\rangle = \pm 1$ depending on the sign of the crossing. This is a simple illustration of a general phenomenon: symmetries, which usually hold for classical links and string links, break down for tangles and virtual links. We will return to this observation in Section 3.

In the next section we introduce Gauss diagram formulas for a family of tangle invariants which includes all Milnor's link-homotopy μ-invariants.

3. Tangle invariants by counting trees

In what follows, let $I = \{i_1, i_2 \ldots, i_r\}$, $1 \le i_1 < i_2 < \cdots < i_r \le n$ and $j \in \{1, 2, \ldots, n\} \setminus I$.

3.1. **Tree diagrams.**

Definition 3.1. A *tree diagram* A with leaves on strings numbered by I and a trunk on j-th string is an arrow diagram which satisfies the following conditions:

- An arrowtail and an arrowhead of an arrow belong to different strings;
- There is exactly one arrow with an arrowtail on i-th string, if $i \in I$, and no such arrows if $i \notin I$;
- All arrows have arrowheads on $I \cup \{j\}$ strings;
- All arrowheads precede the (unique) arrowtail for each $i \in I$, as we follow the i-th strand string in the sense of its orientation.

Note that the total number of arrows in a tree diagram is $r = |I|$; we will call this number the *degree* of A. Our choice of the term tree diagram is explained by the following. Consider A as a graph (with vertices being heads and tails of

arrows and beginning and ending points of the strings). Removing all k-strings where $k \notin I \cup \{j\}$, and cutting off the part of each of the remaining strings after the corresponding arrowtail, we obtain a tree T_A with $r+1$ leaves on the beginning of each i-string with $i \in I \cup \{j\}$ and the root in the endpoint of j-th string. We will also say that T_A is a tree with leaves on I and a trunk on j. See Figure 7, where some tree diagrams with $r = 2$, $j = 1$, $I = \{2, 3\}$ are shown together with corresponding trees.

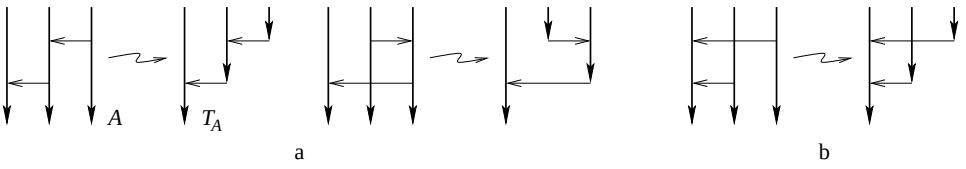

FIGURE 7. Planar and non-planar tree diagrams

Note that every tree T_A could be realized as a planar graph. The tree diagram A is called *planar*, if in its planar realization the order of the leaves coincides with the initial ordering $i_1 < i_2 < \cdots < i_l < j < i_{l+1} < \cdots < i_r$ of the strings as we count the leaves starting from the root clockwise. For example, diagrams in Figure 7a are planar, while the one in Figure 7b is not. Let $\mathcal{A}_{I,j}$ denote the set of all planar tree diagrams with leaves on I and a trunk on j and let $\mathcal{A}_j = \cup_I \mathcal{A}_{I,j}$.

3.2. **Diassociative algebras and trees.** Let the sign of an arrow diagram A be $\mathrm{sign}(A) = (-1)^q$, where q is the number of right-pointing arrows in A. Given a Gauss diagram G of a tangle with the marked j-th string, we define the following quantity, taking value in a free abelian group generated by planar rooted trees[1]:

$$\sum_{A \in \mathcal{A}_j} \mathrm{sign}(A) \langle A, G \rangle \cdot T_A$$

While this formal sum of trees fails to be a tangle invariant, it becomes one modulo certain equivalence relations on trees. These relations turn out to be the axioms of a diassociative algebra (also known as associative dialgebra):

Definition 3.2. ([6]) A diassociative algebra over a ground field k is a k-space V equipped with two k-linear maps

$$\vdash\colon\ V \otimes V \to V \quad \text{and} \quad \dashv\colon\ V \otimes V \to V,$$

called left and right products and satisfying the following five axioms:

$$(2) \qquad \begin{cases} (1) & (x \dashv y) \dashv z = x \dashv (y \vdash z) \\ (2) & (x \dashv y) \dashv z = x \dashv (y \dashv z) \\ (3) & (x \vdash y) \dashv z = x \vdash (y \dashv z) \\ (4) & (x \dashv y) \vdash z = x \vdash (y \vdash z) \\ (5) & (x \vdash y) \vdash z = x \vdash (y \vdash z) \end{cases}$$

Diagrammatically, one can think about a free diassociative algebra as follows. Depict products $a \vdash b$ and $a \dashv b$ as elementary trees shown in Figure 8a. Composition of these operations corresponds then to grafting of trees, see Figure 8b,c.

Axioms (2) correspond to relations on trees shown in Figure 9.

[1]Note that this sum is always finite, since the Gauss diagram contains a fixed number of strings.

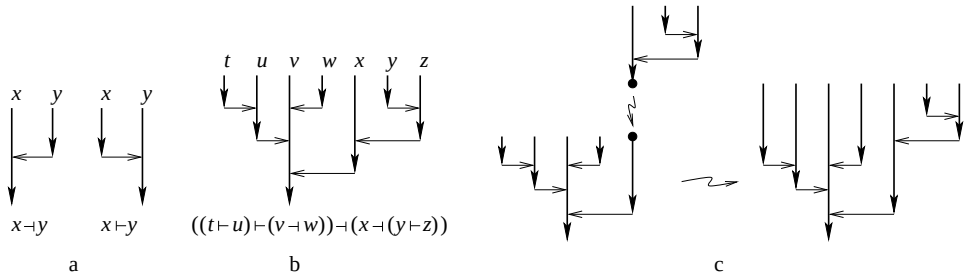

FIGURE 8. Diassociative operations as trees and their compositions

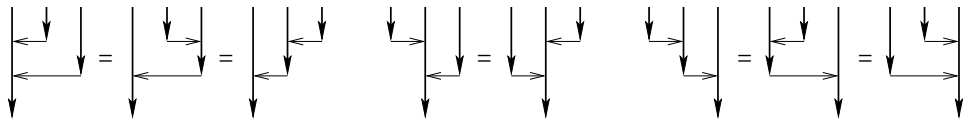

FIGURE 9. Diassociative algebra relations on trees

Denote by $Dias(n)$ the quotient of the vector space generated by planar rooted trees with n leaves by the axioms of the diassociative algebra and let $Dias = \cup_n Dias(n)$. The operadic composition on $Dias$ corresponds to grafting of trees, as illustrated in Figure 8c. See [6] for details.

3.3. **Tree invariants.** Let $[T]$ denote the equivalence class of a planar tree T in $Dias$, and G be the Gauss diagram of a tangle. Then $Z_j(G) \in Dias$ is defined as

$$Z_j(G) = \sum_{A \in \mathcal{A}_j} \text{sign}(A) \langle A, G \rangle [T_A] \tag{3}$$

T_A being the tree corresponding to the tree diagram A. We call $Z_j(G)$ the *tree invariant* of a tangle which has G as its Gauss diagram, since it satisfies the following

Theorem 3.3. *Let L be an ordered (classical or virtual) tangle and let G be a Gauss diagram of L. Then $Z_j(L) = Z_j(G)$ is an invariant of ordered tangles.*

Proof. It suffices to prove that $Z_j(G)$ is preserved under the Reidemeister moves $\Omega 1$–$\Omega 3$ for Gauss diagrams (Figure 5). Given a Gauss diagram G, invariance of $Z_j(G)$ under $\Omega 1$ and $\Omega 2$ follows immediately from the definition of tree diagrams. Indeed, a new arrow appearing in $\Omega 1$ has both its arrowhead and its arrowtail on the same string, so it cannot be in the image of a tree diagram A. Hence the (3) rests intact under the first move. It is also invariant under the second move for the following reason. Two new arrows which appear in $\Omega 2$ have their arrowtails on the same string, so they cannot simultaneously belong to the image of a tree diagram, while maps which contain one of them cancel out in pairs due to opposite signs of the two arrows.

It remains to verify invariance under the third Reidemeister move $\Omega 3$ depicted in Figure 5. Denote by G and G' Gauss diagrams related by $\Omega 3$. Note that there is a bijective correspondence between the summands of $Z_j(G)$ and those of $Z_j(G')$. Indeed, since only the relative position of the three arrows participating in the move changes, all terms which involve only one of these arrows do not change. No terms

involve all three arrows, since such a diagram cannot be a tree diagram. It remains to compare terms which involve exactly two arrows. Note that a diagram which involves two arrows can be a tree diagram only if the fragments participating in the move belong to three different strings. There is a number of cases, depending on the ordering $\sigma_1, \sigma_2, \sigma_3$ of these three strings. Using for simplicity indices $1, 2, 3$ for such an ordering, we can summarize the correspondence of these terms in the table below.

$\sigma_1\,\sigma_2\,\sigma_3$	1 2 3	2 1 3	3 1 2	3 2 1	1 3 2	2 3 1
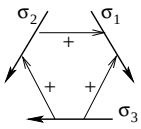	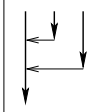	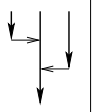	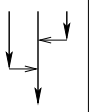	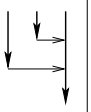	–	–
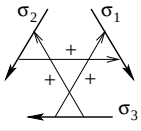	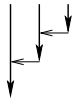	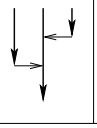	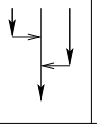	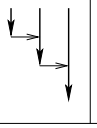	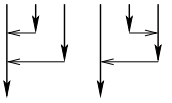	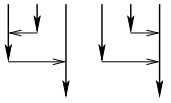

We see that invariance is assured exactly by the diassociative algebra relations, see Figure 9. For four orderings out of six the correspondence is bijective, while for the two last orderings, pairs of trees appearing in the bottom row have opposite signs (due to different number of right-pointing arrows), so their contributions to $Z_j(G')$ cancel out. □

4. Properties of the tree invariants

The tree invariant $Z_j(L)$ takes values in the quotient $Dias$ of the free abelian group generated by trees by the diassociative algebra relations. The equivalence class $[T_A]$ of a tree T_A with trunk on j depends only on the set of its leaves, so it is the same for all arrow diagrams A in the set $\mathcal{A}_{I,j}$ of all planar tree arrow diagrams with leaves on I and trunk on j.

Let $Z_{I,j}$ be the coefficient of Z_j corresponding to trees with leaves on I, namely, $Z_{I,j} = \sum_{A\in\mathcal{A}_{I,j}} \mathrm{sign}(A)\langle A, G\rangle$. For $I = \emptyset$ we set $Z_{\emptyset,j} = 1$.

4.1. **Invariants in low degrees.** Let us start with invariants $Z_{I,j}$ for small values of $r = |I|$.

Counting tree diagrams with one arrow we get

$$Z_{2,1}(L) = \langle \; \text{  } \; , G\rangle \ , \qquad Z_{1,2}(L) = -\langle \; \text{} \; , G\rangle. \tag{4}$$

Note that if L is a string link $Z_{2,1}(L) = -Z_{1,2}(L) = \mathrm{lk}(L_1, L_2)$.

For diagrams with two arrows we obtain

$$Z_{23,1}(L) = \langle \; \text{ 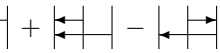 } \; , G\rangle \ , \ Z_{13,2}(L) = -\langle \; \text{  } \; , G\rangle \ , \tag{5}$$

$$Z_{12,3}(L) = \langle \; \text{ 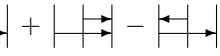 } \; , G\rangle$$

In particular, $Z_{13,2}(L) = Z_{1,2}(L) \cdot Z_{3,2}(L)$. Also, $Z_{12,3}(L) = Z_{23,1}(\bar{L})$, where $\bar{L}$ is the tangle L with reflected ordering $\bar{L}_i = L_{4-i}$ of strings.

Example 4.1. Consider a tangle L with corresponding diagram D_2 depicted in Figure 4 and let us compute $Z_{23,1}(L)$ using formula (5). The corresponding Gauss diagram G_2 contains three subdiagrams of the type  , two of which cancel out, while the remaining one contributes $+1$; there are no subdiagrams of other types appearing in (5). Hence, $Z_{23,1}(L) = 1$.

When an orientation of a component is reversed, invariants $Z_{I,j}$ change sign and jump by a combination of lower degree invariants. For example, denote by L' the 3-string tangle obtained from L by reversal of orientations of L_1. Then,

$$Z_{23,1}(L') = \langle -$$ 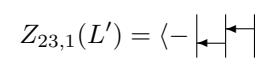 $$, G\rangle.$$

But it is easy to see that $\langle$ 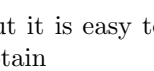 $, G\rangle = \langle$ 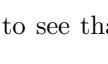 $, G\rangle \cdot \langle$ 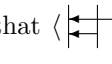 $, G\rangle$, thus we obtain

$$Z_{23,1}(L') = -Z_{23,1}(L) + Z_{2,1}(L) \cdot Z_{3,1}(L).$$

Let us write down explicitly 3-arrow diagrams with trunk on the first string:

(6)

$$Z_{234,1}(L) = \langle$$ 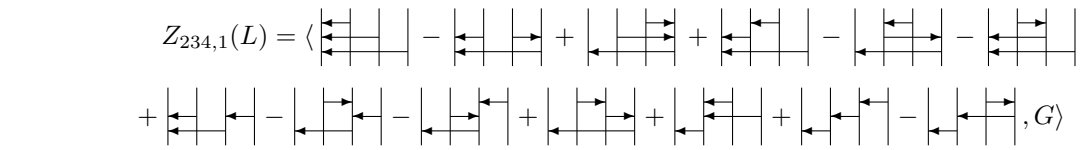 $$, G\rangle$$

For diagrams with trunk on the second or third strings we have $Z_{134,2}(L) = Z_{1,2}(L) \cdot Z_{34,2}(L)$, $Z_{124,3}(L) = Z_{12,3}(L) \cdot Z_{4,3}(L)$. Finally, for $j = 4$ we have $Z_{123,4}(L) = -Z_{432,1}(\bar{L})$, where $\bar{L}$ is obtained from L by the reflection $\bar{L}_i = L_{5-i}$ of the ordering.

4.2. **Elementary properties of tree invariants.** Unlike μ-invariants discussed in Section 2.2 which had simple behavior under change of ordering (see Remark 2.2), tree invariants $Z_{I,j}(L)$ depend significantly on the order of $i_1, \dots, i_r$ and j. Namely, if $L'_i = L_{\sigma(i)}$ for some $\sigma \in S_n$, $\sigma : i \to \sigma(i)$, then, in general, $Z_{I,j}(L')$ is not directly related to $Z_{\sigma(I),\sigma(j)}(L)$. However, in some simple cases dependence of tree invariants on ordering and their behavior under simple changes of ordering and reflections of orientation can be deduced directly from their definition via planar trees:

Proposition 4.2. *Let L be an ordered (classical or virtual) tangle on n stringsand let $I = \{i_1, i_2, \dots, i_r\}$, with $1 \le i_1 < i_2 < \dots < i_r \le n$.*

(1) *For $1 < k < r$ we have*

$$Z_{I \smallsetminus i_k, i_k}(L) = Z_{I_k^-, i_k}(L) \cdot Z_{I_k^+, i_k}(L)$$

where $I_k^- = I \cap [1, i_k - 1] = \{i_1, \dots, i_{k-1}\}$ and $I_k^+ = I \cap [i_k + 1, n] = \{i_{k+1}, \dots, i_r\}$.

(2) *Denote by $\bar{L}$ the tangle L with reflected ordering: $\bar{L}_i = L_{\bar{i}}$, $i = 1, \dots, n$, where $\bar{i} = n + 1 - i$, so $\bar{I} = \{\bar{i_r}, \dots, \bar{i_2}, \bar{i_1}\}$. Then*

$$Z_{I,j}(\bar{L}) = (-1)^r Z_{\bar{I},\bar{j}}(L)$$

(3) *Finally, denote by L^σ the tangle the tangle obtained from L by cyclic permutation $\sigma = (i_1 i_2 \dots i_r)$ of strings of L (that is, $L^\sigma_{i_k} = L_{i_{k+1}}$ for $k = 1, \dots, r-1$ and $L^\sigma_{i_r} = L_{i_1}$), followed by the reversal of orientation of the last string $L^\sigma_{i_r} = L_{i_1}$. Then*

$$Z_{I \smallsetminus i_r, i_r}(L^\sigma) = Z_{I \smallsetminus i_1, i_1}(L)$$

Proof. Indeed, a planar tree with trunk on j consists of the "left half-tree" with leaves on $I \cap [1, j-1]$ and the "right half-tree" with leaves on $I \cap [j+1, n]$. Thus the first equality follows directly from the definition of the invariants.

Also, the reflection $i \mapsto \bar{i}$ of ordering simply reflects a planar tree with respect to its trunk, exchanging the left and the right half-trees and changing all right-pointing arrows into left-pointing ones and vice versa, so the second equality follows (since the total number of arrows is r).

Finally, let us compare planar tree subdiagrams in the Gauss diagram G of L and in the corresponding Gauss diagram G^σ of L^σ. Cyclic permutation σ of ordering, followed by the reversal of orientation of the trunk, establishes a bijective correspondence between planar tree diagrams with leaves on $I \smallsetminus i_1$ and trunk on i_1 and planar tree diagrams with leaves on $I \smallsetminus i_r$ and trunk on i_r. Given a diagram $A \in \mathcal{A}_{i_1}$, we can obtain the corresponding diagram $A^\sigma \in \mathcal{A}_{i_r}$ in two steps: (1) redraw the trunk i_1 of A on the right of all strings, with an upwards orientation; (2) reverse the orientation of the trunk so that it is directed downwards. See Figure 10. Signs of these diagrams are related as follows: $\operatorname{sign}(A) = (-1)^q \operatorname{sign}(A^\sigma)$, where

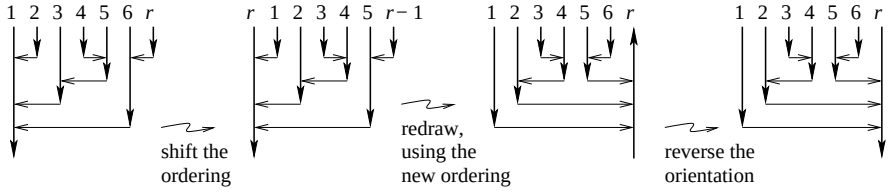

FIGURE 10. Reordering strings and reversing the orientation of the trunk

q is the number of arrows with arrowheads on the trunk (since all such arrows become right-pointing instead of left-pointining). Now note that when we pass from G to G^σ, the reflection of orientation of $L^\sigma_{i_r}$ has similar effect on the signs of arrows, namely, the sign of each arrow in G^σ with one end on the trunk (and the other end on some other string) is reversed, so $\langle A, G\rangle = (-1)^q \langle A^\sigma, G^\sigma\rangle$. These two factors of $(-1)^q$ cancel out to give $\operatorname{sign}(A)\langle A, G\rangle = \operatorname{sign}(A^\sigma)\langle A^\sigma, G^\sigma\rangle$ and the last statement follows. □

Tree invariants $Z_{I,j}(L)$ satisfy the following skein relations. Let L_+, L_-, L_0 and L_∞ be four tangles which differ only in the neighborhood of a single crossing d, where they look as shown in Figure 11. In other words, L_+ has a positive crossing, L_- has a negative crossing, L_0 is obtained from $L_\pm$ by smoothing, and L_∞ is obtained from $L_\pm$ by the reflection of orientation of L_{i_k}, followed by smoothing. Orders of strings of $L_\pm$, L_0 and L_∞ coincide in the beginning of each string. See Figures 11 and 12. We will call $L_\pm$, L_0 and L_∞ a *skein quadruple*.

Theorem 4.3. *Let $j < i_1 < i_2 < \dots < i_r$ and $1 \le k \le r$. Let L_+, L_-, L_0 and L_∞ be a skein quadruple of tangles on n strings which differ only in the neighborhood of*

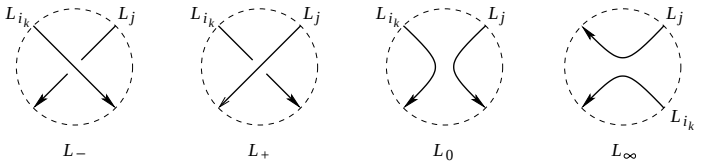

FIGURE 11. Skein quadruple of tangles

a single crossing d of j-th and i_k-th components, see Figure 11. For $m = 1, \dots, k$ denote $I_m^- = \{i_1, \dots, i_{m-1}\}$, $I_m^+ = I \smallsetminus I_m^- \smallsetminus i_k = \{i_m, \dots, i_{k-1}, i_{k+1}, \dots, i_r\}$. Then

$$Z_{I,j}(L_+) - Z_{I,j}(L_-) = Z_{I_k^-,j}(L_\infty) \cdot Z_{I_k^+,i_k}(L_0) \ ; \tag{7}$$

$$Z_{I,j}(L_+) - Z_{I,j}(L_-) = \sum_{m=1}^{k} Z_{I_m^-,j}(L_\pm) \cdot Z_{I_m^+,i_k}(L_0) \ . \tag{8}$$

Here we used the notation $Z_{I_m^-,j}(L_\pm)$ to stress that $Z_{I_m^-,j}(L_+) = Z_{I_m^-,j}(L_-)$.

Remark 4.4. Note that for $m = 1$ we have $I_1^- = \emptyset$ and $I_1^+ = I \smallsetminus i_k$, which corresponds to the summand $Z_{I \smallsetminus i_k, i_k}(L_0)$ in the right hand side of (8). Also, in the particular case $k = 1$ both of the equations (7),(8) simplify to

$$Z_{I,j}(L_+) - Z_{I,j}(L_-) = Z_{I \smallsetminus i_1, i_1}(L_0) \qquad (k = 1) \tag{9}$$

Finally, for $k = r$ equation (7) becomes

$$Z_{I,j}(L_+) - Z_{I,j}(L_-) = Z_{I \smallsetminus i_r, j}(L_\infty) \qquad (k = r)$$

Example 4.5. Consider the tangle $L = L_+$ depicted in Figure 12 and let us compute $Z_{23,1}(L)$. Notice that if we switch the indicated crossing of L_1 with L_2 to the negative one, we get the link L_- with L_3 unlinked from L_1 and L_2, so $Z_{23,1}(L_-) = 0$. We have $i_1 = 2, i_2 = 3$ and $k = 1$, thus we can use equation (9) and get

$$Z_{23,1}(L) = Z_{23,1}(L) - Z_{23,1}(L_-) = Z_{3,2}(L_0) = 1,$$

in agreement with the calculations of Example 4.1.

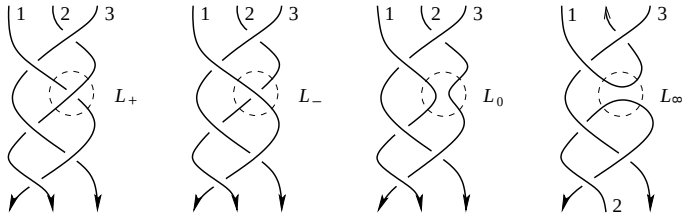

FIGURE 12. Computation of $Z_{23,1}$ for Borromean rings

Proof. To prove Theorem 4.3 consider Gauss diagrams G_ε of L_ε, $\varepsilon = \pm$ in a neighborhood of the arrow $a_\pm$ corresponding to the crossing d of $L_\pm$, see Figure 13a.

Here if L_j passes under L_{i_k} in the crossing d of L_+ $\varepsilon = +$, and $\varepsilon = -$ otherwise. There is an obvious bijective correspondence between tree subdiagrams of G_+ and G_- which do not include $a_\pm$, so these subdiagrams cancel out in pairs in

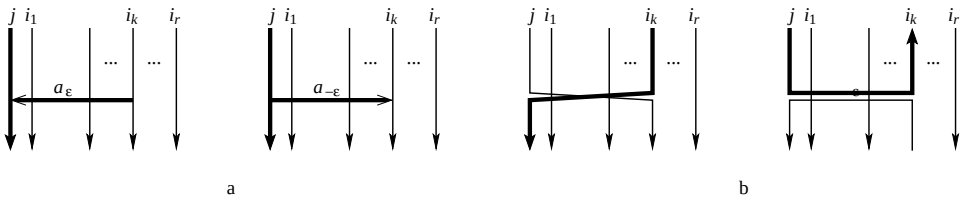

FIGURE 13. Gauss diagrams which appear in skein relations

$\langle A, G_+\rangle - \langle A, G_-\rangle$. Since we count only trees with the root on j-th string, the only subdiagrams which contribute to $Z_{I,j}(L_+) - Z_{I,j}(L_-)$ are subdiagrams of G_+ which contain a_+ if $\varepsilon = +$, and subdiagrams of G_- which contain a_- if $\varepsilon = -$. Note that in each case the arrow $a_\pm$ is counted with the positive sign (since if $\varepsilon = -1$, it appears in $-Z_{I,j}(L_-)$). Without loss of generality we may assume that $\varepsilon = +$. Thus,

$$Z_{I,j}(L_+) - Z_{I,j}(L_-) = \sum_{A \in \mathcal{A}_{I,j}} \langle A, G_+\rangle_{a_+} \ ,$$

where $\langle A, G\rangle_a$ denote the sum of all maps $\phi : A \to G$ such that $a \in \mathrm{Im}(\phi)$. See the left hand side of Figure 14.

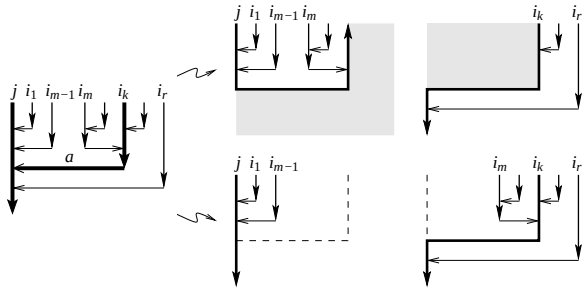

FIGURE 14. Skein relations on Gauss diagrams

Interpreting L_0 and L_∞ in terms of Gauss diagrams as shown in Figure 13b, and using Proposition 4.2, we immediately get equality (7). See the top row of Figure 14.

Subdiagrams which appear in the equality (8) are shown in the bottom row of Figure 14. To establish (8), it remains to understand why subdiagrams which contain arrows with arrowheads on j under a_+ cancel out in $\sum_{m=1}^{k} Z_{I^-_m,j}(L_\pm) \cdot Z_{I^+_m,i_k}(L_0)$. Fix $1 \le m \le k$ and let $A_1 \in \mathcal{A}_{I^-_m,j}$ and $A_2 \in \mathcal{A}_{I^+_m,i_k}$ be two tree arrow diagrams together with maps $\phi_1 : A_1 \to G_+$, $\phi_2 : A_2 \to G_0$. Suppose that one of the subdiagrams $G_1 = \mathrm{Im}(\phi_1(A_1))$ and $G_2 = \mathrm{Im}(\phi_2(A_2))$ of G_+ contains an arrow, which ends on j-th string under a. Denote by a_{bot} the lowest such arrow in $G_1 \cup G_2$ (as we follow j-th string along the orientation). Without loss of generality, we may assume that it belongs to G_1. See Figure 15. Since a_{bot} ends on the common part of the trunks of G_+ and G_0, we may rearrange pieces of G_1 to get two different tree diagrams with the same set of arrows as $G_1 \cup G_2$. Namely, removal of a_{bot} from G_1 splits it into two connected components G_1' and G_1'', so that G_1' contains strings $j, i_1, \dots, i_{s-1}$ and G_1'' contains strings $i_s, \dots, i_{m-1}$ for some $1 \le s \le m$.

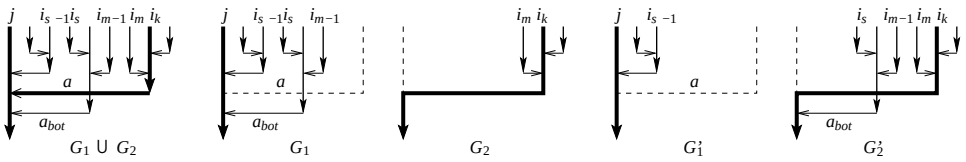

FIGURE 15. Cancelation of subdiagrams with arrows under a

Then G_1' is a tree subdiagram of G_+ (with trunk on j and leaves on I_s^-), and $G_2' := G_1'' \cup a_{bot} \cup G_2$ is a tree subdiagram of G_0 (with the trunk on i_k and leaves on I_s^+). See Figure 15. Their contribution to $Z_{I_s^-,j}(L_\pm) \cdot Z_{I_s^+,i_k}(L_0)$ cancels out with that of G_1 and G_2 to $Z_{I_m^-,j}(L_\pm) \cdot Z_{I_m^+,i_k}(L_0)$. Indeed, while $G_1' \cup G_2'$ contain the same set of arrows as $G_1 \cup G_2$, the arrow a_{bot} is now right-pointing, so it is counted with additional factor of -1. This completes the proof of the theorem. □

4.3. **Identification with Milnor's μ-invariants.** It turns out, that for $j < i,\ \forall i \in I$, the tree invariant $Z_{I,j}$ coincides with a Milnor's μ-invariant:

Theorem 4.6. *Let L be an ordered (classical or virtual) tangle on n strings and let $1 \le j < i_1 < i_2 < \cdots < i_r \le n$. Then*

$$Z_{I,j}(L) = \mu_{i_1 \dots i_r, j}(L)$$

Proof. Theorem 3.1 of [8] (together with Remark 2.2) implies that $\mu_{i_1 \dots i_r, j}(L)$ satisfies the same skein relation as (7), that is

$$\mu_{I,j}(L_+) - \mu_{I,j}(L_-) = \mu_{I_k^-,j}(L_\infty) \cdot \mu_{I_k^+,i_k}(L_0)\ .$$

Moreover, these invariants have the same normalization $Z_{I,j}(L) = \mu_{I,j}(L) = 0$ for any tangle L with the j-th string passing in front of all other strings. The skein relation and the normalization completely determines the invariant. □

Corollary 4.7. *Formulas* (5) *and* (6) *define invariants $\mu_{23,1}$ and $\mu_{234,1}$ respectively.*

Example 4.8. If we return to the tangle L of Examples 4.1 and 4.5, shown in Figure 12, we get $\mu_{23,1}(L) = Z_{23,1} = 1$, in agreement with the fact that the closure $\widehat{L}$ of L is the Borromean link.

Remark 4.9. Note that in the proof of Theorem 3.3 we did not use the realizability of Gauss diagrams in our verification of invariance of tree invariants under Reidemeister moves in Figure 5, so Theorems 3.3 and 4.6 hold for virtual tangles as well. Recall, however, that in the virtual case there is an alternative definition of "lower" μ-invariants of virtual tangles via the lower tangle group, see Section 2.4. To recover these invariants using Gauss diagram formulas we simply reverse directions of all arrows in the definition of the set of tree diagrams $\mathcal{A}_j$.

5. Operadic structure of the invariants

5.1. **Tree tangles.**

Definition 5.1. A tree tangle L is a $(k,1)$-tangle without closed components. The string ending on the bottom (that is, on $D^2 \times \{0\}$) is called the trunk of L.

We will assume that tree tangles are oriented in such a way that the trunk starts at the top $D^2\times\{1\}$ and ends on the bottom $D^2\times\{0\}$ of C. To simplify the notation, for a tree tangle L with the trunk on the j-th string we will denote $Z_j(L)$ by $Z(L)$. There is a natural way to associate to a (k,l)-tangle with a distinguished string a tree tangle by pulling up all but one of its strings. Namely, suppose that the j-th string of a (k,l)-tangle L starts at the top and ends on the bottom. Then L can be made into a tree $(k+l-1,1)$-tangle $\widehat{L}_j$ with the trunk on j-th string by the operation of $j-$capping shown in Figure 16.

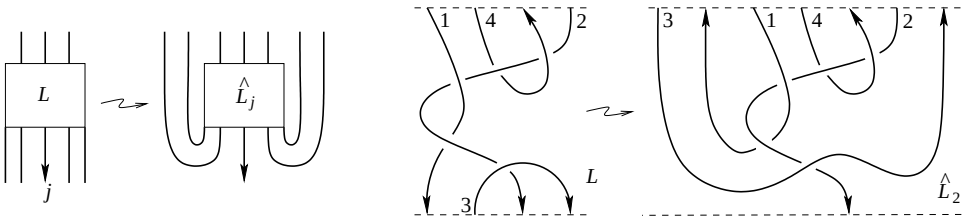

FIGURE 16. Capping a tangle

Gauss diagrams of L and $\widehat{L}_j$ are the same (since crossings of $\widehat{L}_j$ are the same as in L), so their tree invariants coincide: $Z_j(L)=Z(\widehat{L}_j)$.

5.2. **Operadic structure on tree tangles.** Denote by $\mathcal{T}(n)$ the set of tree tangles on n strings. Tree tangles form an operad $\mathcal{T}$. The operadic composition

$$\mathcal{T}(n)\times\mathcal{T}(m_1)\times\cdots\times\mathcal{T}(m_n)\to\mathcal{T}(m_1+\cdots+m_n)$$

is defined as follows. A partial composition $\circ_i:\mathcal{T}(n)\times\mathcal{T}(m)\to\mathcal{T}(n+m-1)$ corresponds to taking the satellite of the i-th component of a tangle:

Definition 5.2. Let $L\in\mathcal{T}(n)$ and $L'\in\mathcal{T}(m)$ be tree tangles, and let $1\le i\le n$. Define the satellite tangle $L\circ_i L'\in\mathcal{T}(n+m-1)$ as follows. Cut out of $C=D^2\times[0,1]$ a tubular neighborhood $N(L_i)$ of the i-th string L_i of L. Glue back into $C\smallsetminus N(L_i)$ a copy of a cylinder C which contains L', identifying the boundary $\partial D^2\times[0,1]$ with the boundary of $N(L_i)$ in $C\smallsetminus N(L_i)$ using the zero framing[2] of L_i. See Figure 17. Reorder components of the resulting tree tangle appropriately.

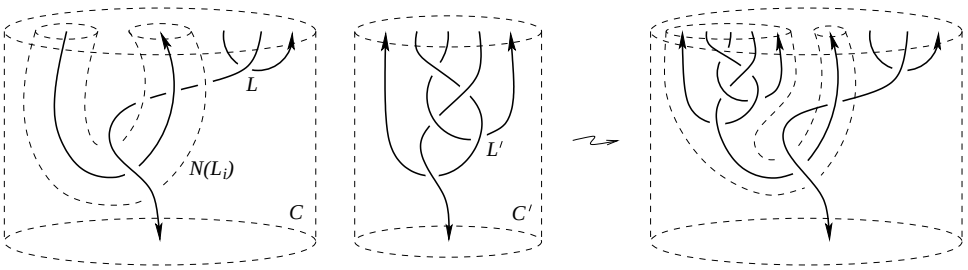

FIGURE 17. The satellite $L\circ_i L'$ of the i-th string of the tree tangle L

[2]In fact, the result does not depend on the framing since only one component of L' ends on the bottom of the cylinder.

Now, given a tangle $L \in \mathcal{T}(n)$ and a collection of n tree tangles $L^1 \in \mathcal{T}(m_1),\dots,$ $L^n \in \mathcal{T}(m_n)$, we define the composite tangle $L(L^1,\dots,L^n) \in \mathcal{T}(m_1+\dots+m_n)$ by taking the relevant satellites of all components of L (and reordering the components of the resulting tangle appropriately).

The following theorem follows directly from the definition of the operadic structure on $\mathcal{T}$ and the construction of the map Z from tangles to diassociative trees given by equation (3), Section 3.3.

Theorem 5.3. *The map $Z : \mathcal{T} \to Dias$ is a morphism of operads.*

References

[1] S.Chmutov, S.Duzhin, J.Mostovoy. *Introduction to Vassiliev knot invariants.* Draft, September 9, 2010, 514pp, http://www.pdmi.ras.ru/∼duzhin/papers/cdbook/

[2] M. Goussarov, M. Polyak, O. Viro, *Finite type invariants of virtual and classical knots*, Topology **39** (2000), 1045–1068.

[3] N. Habegger, X.-S. Lin, *The classification of links up to link-homotopy*, J. Amer. Math. Soc. **3** (1990), 389–419.

[4] L. Kauffman, *Virtual knot theory*, European J. Combin. **20** (1999), no. 7, 663–690.

[5] J. Levine, *The $\bar{\mu}$-invariants of based links*, In: Differential Topology, Proc. Siegen 1987 (ed. U.Koschorke), Lect. Notes **1350**, Springer-Verlag, 87–103.

[6] J.-L. Loday, *Dialgebras,* In: Dialgebras and related operads, 7–66, Lecture Notes in Math., 1763, Springer, Berlin, 2001.

[7] J. Milnor, *Link groups*, Annals of Math. **59** (1954), 177–195; *Isotopy of links*, Algebraic geometry and topology, A symposium in honor of S.Lefshetz, Princeton Univ. Press (1957).

[8] M. Polyak, *Skein relations for Milnor's μ-invariants*, Alg. Geom. Topology **5** (2005), 1471–1479.

[9] M. Polyak, *Minimal generating sets of Reidemeister moves*, Quantum Topology **1** (2010), 399–411.

[10] M. Polyak, O. Viro, *Gauss diagram formulas for Vassiliev invariants*, Int. Math. Res. Notices **11** (1994), 445–454.

Université de Lyon, Université Lyon 1, ICJ, UMR 5208 CNRS, 43 blvd 11 novembre 1918, 69622 Villeurbanne CEDEX, France

E-mail address: okra@math.univ-lyon1.fr

Department of mathematics, Technion, Haifa 32000, Israel

E-mail address: polyak@math.technion.ac.il